



Supporting Information

# Ag-Activated Metal–Organic Framework with Peroxidase-like Activity Synergistic Ag<sup>+</sup> Release for Safe Bacterial Eradication and Wound Healing

Jie Zhou <sup>1,2,†</sup>, Ning Chen <sup>3,4,†</sup>, Jing Liao <sup>2,3,†</sup>, Gan Tian <sup>5</sup>, Linqiang Mei <sup>2</sup>, Guoping Yang <sup>1,\*</sup>, Qiang Wang <sup>3,\*</sup> and Wenyan Yin <sup>2,\*</sup>

<sup>1</sup> Jiangxi Key Laboratory for Mass Spectrometry and Instrumentation, Jiangxi Province Key Laboratory of Synthetic Chemistry, East China University of Technology, Nanchang 330013, China

<sup>2</sup> CAS Key Laboratory for Biomedical Effects of Nanomaterials and Nanosafety, Institute of High Energy Physics, Chinese Academy of Sciences, Beijing 100049, China

<sup>3</sup> Laboratory for Micro-Sized Functional Materials, Department of Chemistry and College of Elementary Education, Capital Normal University, Beijing 100048, China

<sup>4</sup> School of Energy and Chemical Engineering, Ulsan National Institute of Science and Technology (UNIST), Ulsan 44919, Republic of Korea

<sup>5</sup> Institute of Pathology, The First Affiliated Hospital, Third Military Medical University, Chongqing 400038, China

\* Correspondence: erick@ecut.edu.cn (G.Y.); qwchem@gmail.com (Q.W.); yinwy@ihep.ac.cn (W.Y.); Tel.: +86-18800173887 (G.Y.); +86-13811227118 (Q.W.); +86-18511550963 (W.Y.)

† These authors contributed equally to this work.

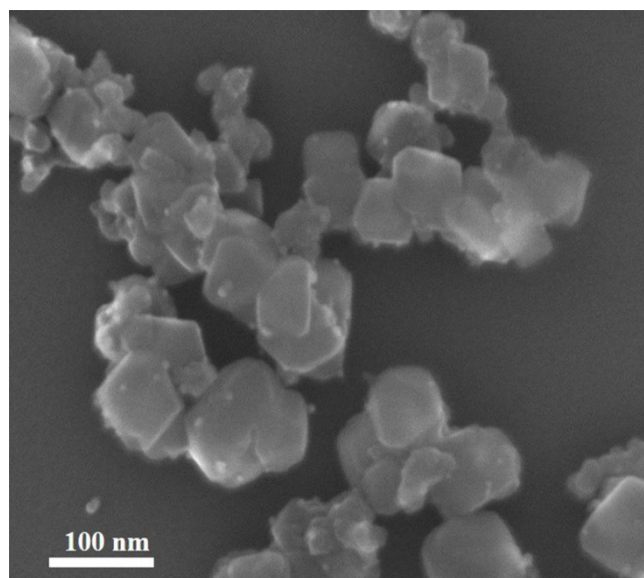
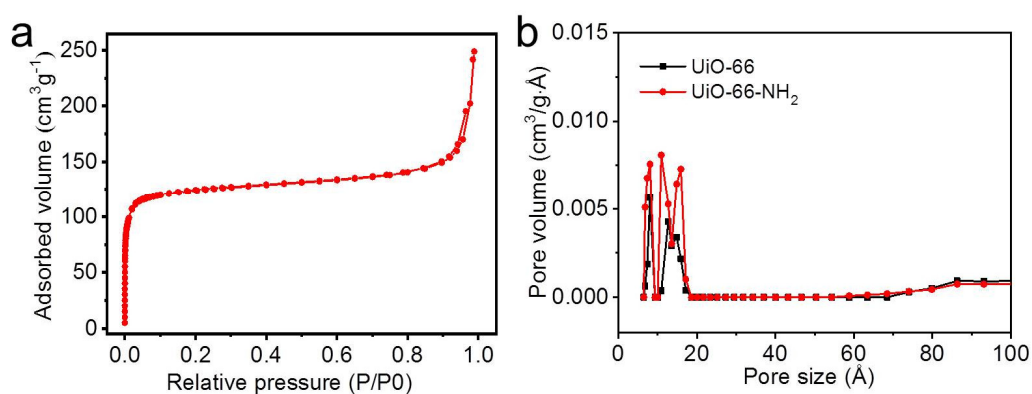
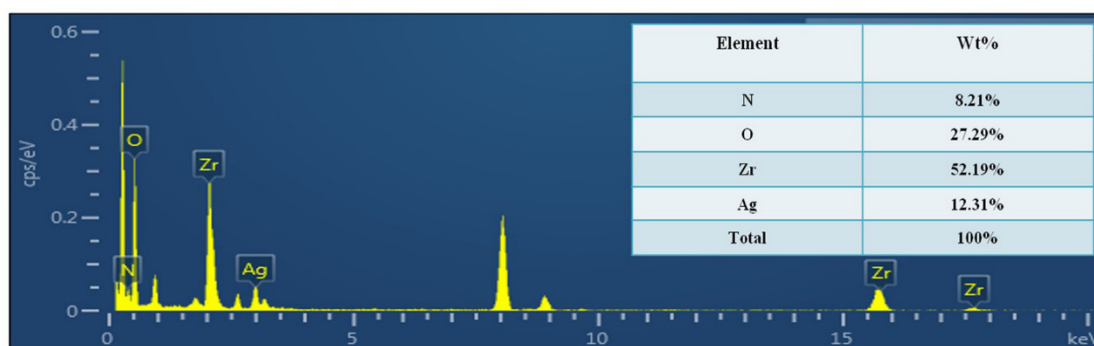


Figure S1. FE-SEM image of UiO-66-NH<sub>2</sub>-Ag nanocomposite.



**Figure S2.** (a)  $\text{N}_2$  adsorption/desorption isotherms of UiO-66-NH<sub>2</sub> and (b) BJH pore size distribution curves of UiO-66 and UiO-66-NH<sub>2</sub>.



**Figure S3.** EDX of UiO-66-NH<sub>2</sub>-Ag nanocomposite. Inset is the mass ratio of different elements.

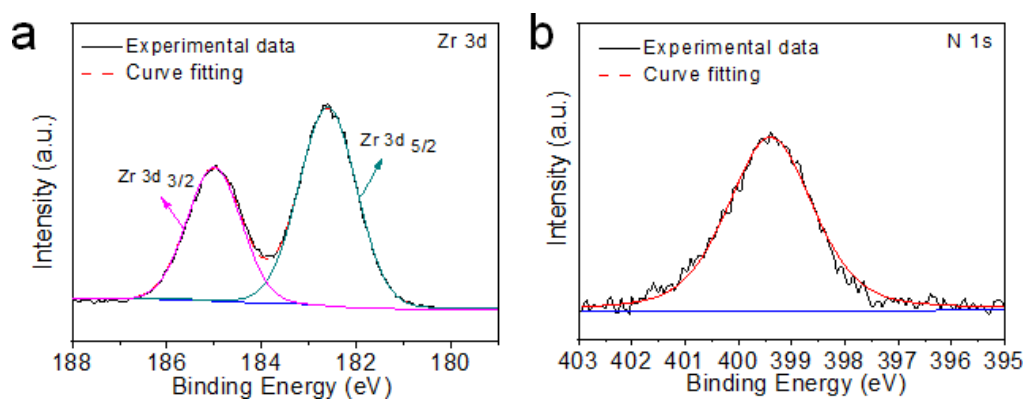


**Figure S4.** XPS data of high-resolution (a) Zr 3d and (b) N 1s of UiO-66-NH<sub>2</sub>-Ag nanocomposite.

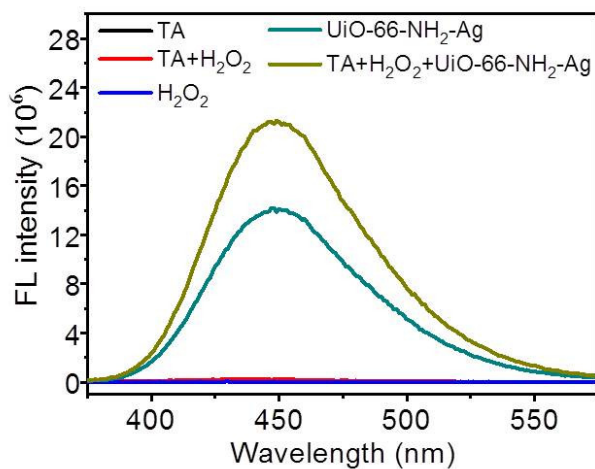


Figure S5. FL spectra of TAOH after different treatments.

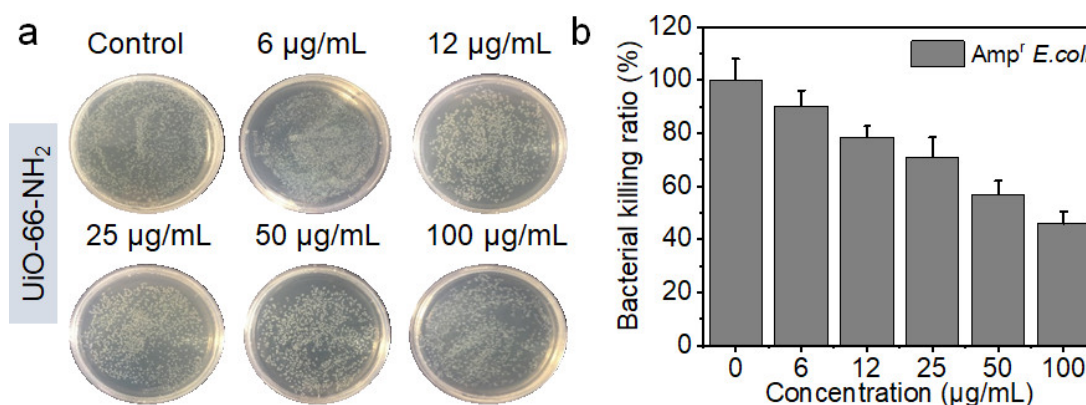


Figure S6. (a) Photographs of bacterial colonies formed by *Amp<sup>r</sup> E. coli* exposed to different concentrations of UiO-66-NH<sub>2</sub>. (b) *Amp<sup>r</sup> E. coli* killing ratio treated with different concentrations of UiO-66-NH<sub>2</sub>.

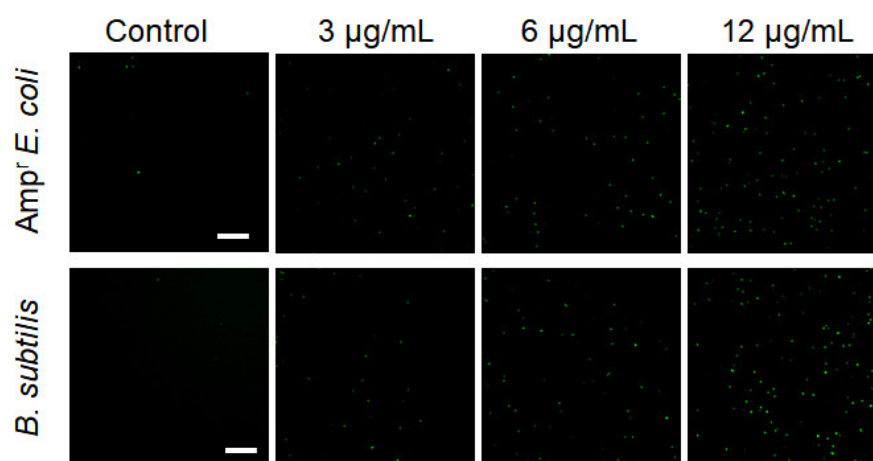
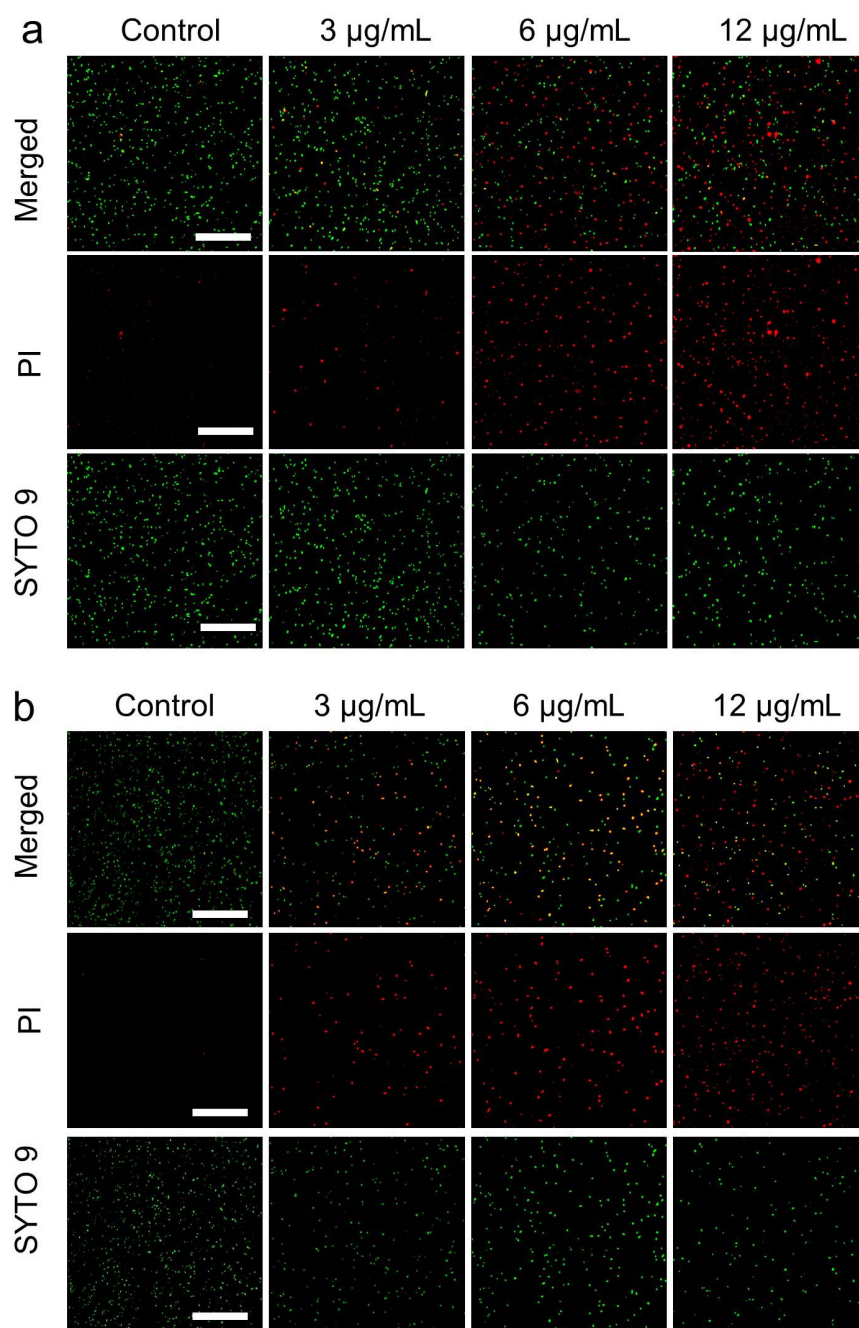
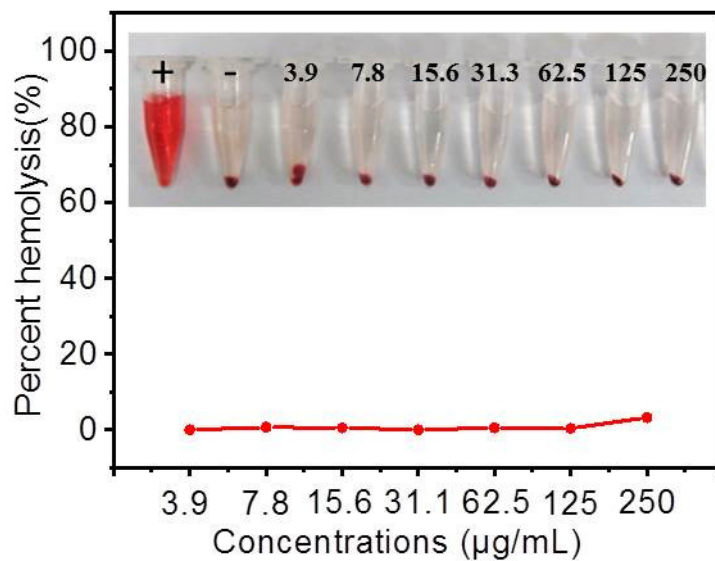


Figure S7. Fluorescence images of *Amp<sup>r</sup> E. coli* and *B. subtilis* incubated with different concentrations of UiO-66-NH<sub>2</sub>-Ag using DCFH-DA probe for ROS detection. Scale bars: 50 μm.



**Figure S8.** Fluorescence images of (a) *Amp<sup>r</sup> E. coli* and (b) *B. subtilis* treated with different concentrations of UiO-66-NH<sub>2</sub>-Ag incubated with SYTO-9 and PI. Scale bars: 100  $\mu\text{m}$ .



**Figure S9.** Hemolysis experiment of UiO-66-NH<sub>2</sub>-Ag at different concentrations. Inset is the corresponding photograph of the UiO-66-NH<sub>2</sub>-Ag at different concentrations.

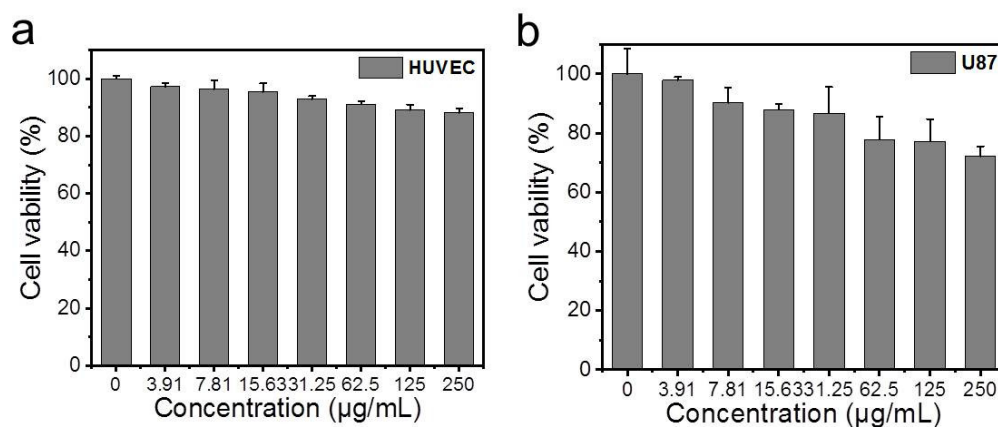


**Figure S10.** Cell viabilities of (a) HUVEC and (b) U87 cells after incubation with different concentrations of UiO-66-NH<sub>2</sub>-Ag for 24 h.

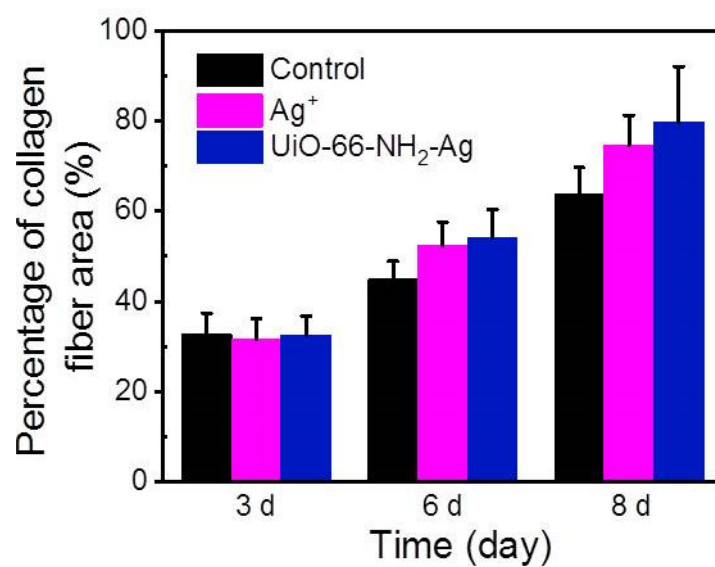


Figure S11. Percentage of collagen fiber area after different treatments during treatment.

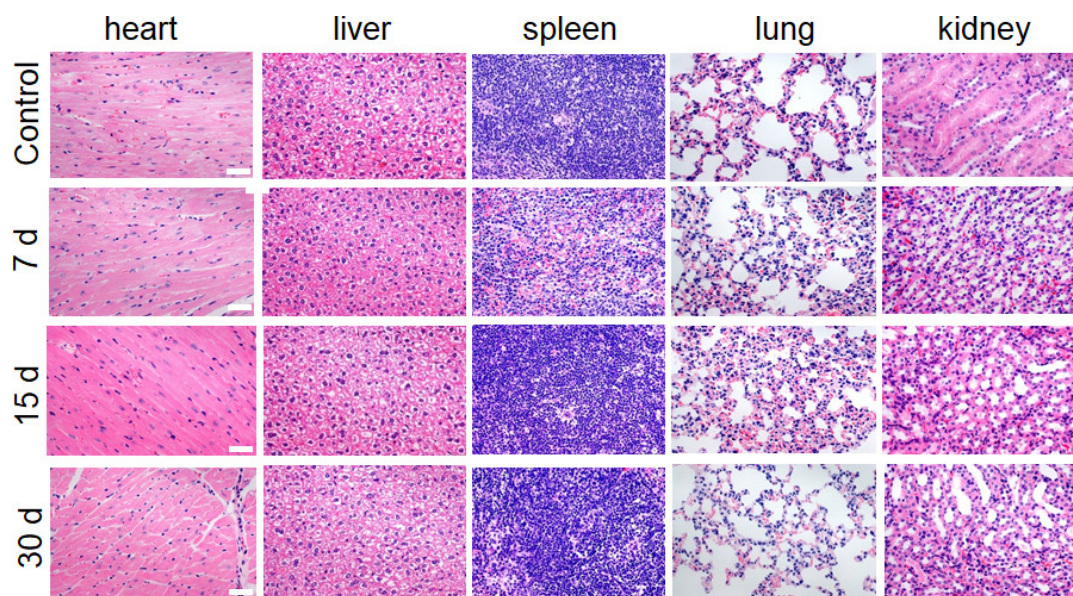
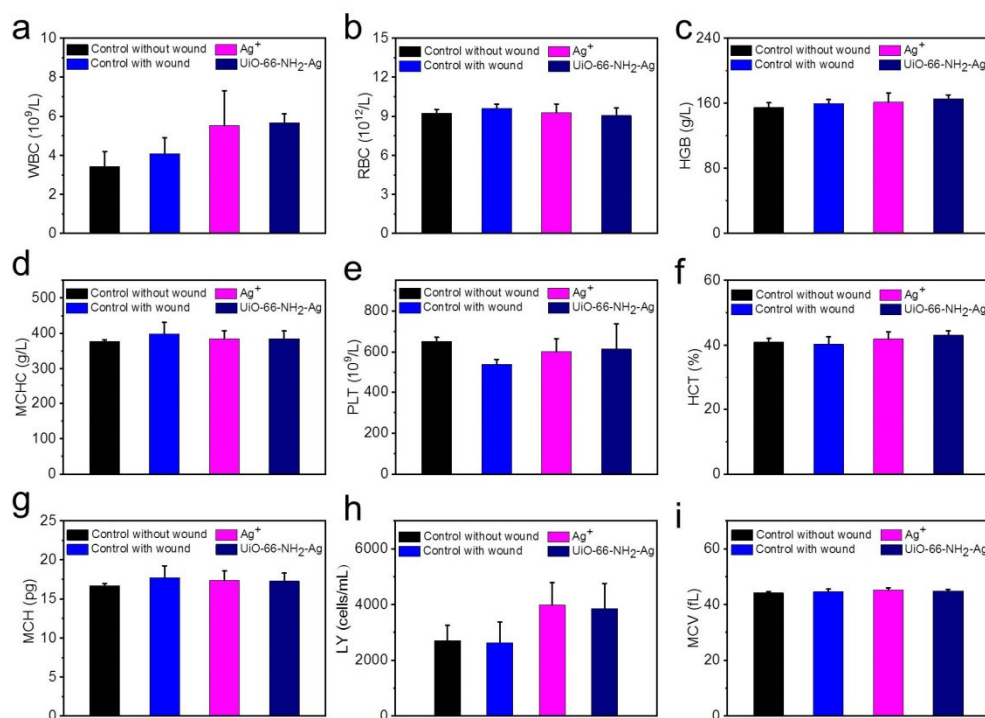


Figure S12. Representative H&E stained images of major organs of mice after treated with UiO-66-NH<sub>2</sub>-Ag for different days. Scale bars: 20  $\mu$ m.



**Figure S13.** Routine blood analysis of mice after 8 days of treatment. The results show the (a) white blood cell (WBC), (b) red blood cell (RBC), (c) hemoglobin (HGB), (d) mean corpuscular hemoglobin concentration (MCHC), (e) platelets (PLT), (f) hematocrit (HCT), (g) mean corpuscular hemoglobin (MCH), (h) lymphocyte (LY) and (i) mean corpuscular volume (MCV) in each group.